Journal of Materials Science: Materials in Electronics (2020) 31:11470–11481
https://doi.org/10.1007/s10854-020-03695-y

Effects of the Ni(P) plating thickness on microstructure evolution of interfacial IMCs in Sn–58Bi/Ni(P)/Cu solder joints

Jinxuan Cheng[1] · Xiaowu Hu[1] · Zhe Zhang[1] · Qinglin Li[2]

Received: 16 April 2020 / Accepted: 26 May 2020 / Published online: 29 May 2020
© Springer Science+Business Media, LLC, part of Springer Nature 2020

Abstract

Effects of the Ni(P) plating thickness on interfacial reaction in the Sn–58Bi/Ni(P)/Cu joint system were revealed. It was found that the interfacial reaction was significantly influenced by the thickness of Ni(P) plating, and 0.1 µm Ni(P) plating completely transformed into Ni_2SnP layer after soldering. This Ni_2SnP layer not only provided a large number of diffusion channels but also reduced the solder joint reliability, demonstrating that 0.1 µm Ni(P) plating was not efficient in inhibiting the diffusion process between solder and substrate. However, the Ni(P) plating with thickness more than 0.5 µm could effectively inhibit atomic diffusion, and the Sn–Ni interaction would dominate the interfacial reaction instead of Cu–Sn phases. Although the Ni(P) plating with thickness of 0.5 µm partly transformed into Ni_2SnP layer, the growth rate of compound layer was suppressed. In addition, the Ni_3Sn_4 would transform into $(Cu,Ni)_6Sn_5$ since Ni_2SnP layer provided channels for Cu diffusing toward the solder/Ni_3Sn_4 interface. The Ni(P) plating with thickness of 1.5 µm remained integrated even after aging for 240 h, nonetheless, the excessive thickness of this barrier was unnecessary. Thus, it could be concluded that the appropriate thickness of Ni(P) plating should be controlled at 0.5–1.5 µm.

1 Introduction

Recently, the microelectronic packing industry has developed rapidly, and there was an urgent need for reliable Cu–Sn solder joints. A reliable solder joint could not only provide electrical connection, but also guarantee mechanical connection for electronic products [1, 2]. As well known, the reliability of solder joints was determined by the composition and thickness of the intermetallic compound (IMC). Therefore, the reliability of solder joint can be evaluated via observing the growth of the IMC [3]. In the past few decades, Sn–Pb solder used to be widely employed in microelectronic packing due to its excellent mechanical properties and wettability [4–6]. However, several Sn-based solders, such as Sn–Ag, Sn–Bi, Sn–Ag–Cu solder, have replaced Sn–Pb solder owing to much concern for the environment and health [7, 8]. Among them, the Sn–58Bi eutectic solder with low melting point was particularly suitable for connecting electronic devices, which were susceptible to high temperature damage [9, 10].

In general, the interfacial reaction between Cu substrate and Sn-based solder occurred rapidly and formed the overgrow IMC, which resulted in reduction of the joint reliability [11, 12]. Electroless Ni(P) layer has been extensively used in soldering as a diffusion barrier layer between solder and substrate. According to previous studies, the reaction rate between Sn–Ni was much slower than that between Sn–Cu [2, 13]. During soldering, Ni atoms in the Ni(P) plating would react with Sn-based solder, forming Ni–Sn compound such as Ni_3Sn_4, Ni_2Sn and so on. Meanwhile, P atoms in the Ni(P) plating accumulated at the interface between Ni–Sn compound and substrate to form a P-rich layer (Ni_3P or Ni_2SnP) [14]. Besides, it has been reported that the thickness of Ni(P) plating had a significant influence on the reliability of solder joints [15–18].

During the soldering process, the Ni(P) plating with suitable thickness was regarded as a protective layer and a diffusion barrier. And in previous studies, effects of Ni(P) plating thickness on the interaction between Sn–3Ag–0.5Cu solder and Electroless Ni(P)/Electroless Pd/Immersion Au (ENEPIG) have been investigated. Ho et al. [2] found that P-rich layer formed between the IMC and substrate when

✉ Xiaowu Hu
huxiaowu@ncu.edu.cn

[1] School of Mechanical & Electrical Engineering, Nanchang University, Nanchang 330031, China

[2] State Key Laboratory of Advanced Processing and Recycling of Nonferrous Metals, Lanzhou University of Technology, Lanzhou 730050, People's Republic of China

the thickness of Ni(P) plating exceeded 0.18 μm. Besides, the growth of Cu_6Sn_5 and Cu_3Sn IMCs was suppressed with the formation of P-rich IMC layer. Meanwhile, Ho et al. [19] also confirmed that the growth of Ni_2SnP layer could inhibit the formation of $(Cu,Ni)_6Sn_5$. Furthermore, Ho et al. [15] confirmed that the interaction would transform from Cu–Sn into Sn–Ni when the Ni(P) plating thickness increased from 0 to 7 μm. And the shear strength decreased with increase of the Ni(P) plating thickness. Hong et al. [20] found that the $(Cu,Ni)_6Sn_5$ IMC layer formed at the bottom and top sides of the interface regardless of the Ni(P) plating thickness and aging condition. Furthermore, the shear strength of the solder joint hardly changed when the plating thickness increased from 0.7 to 1.0 μm. Although the interaction between solder and Ni(P) plating thicker than 3.9 μm has been reported [21], it was still lacking research about the interfacial reaction between solder and Ni(P) plating with different thickness. Therefore, the purpose of this study was to investigate effects of Ni(P) plating thickness on the interfacial reaction in Sn–58Bi based joint systems.

2 Experimental procedures

The Cu plates were cut into the size of $10 \times 10 \times 2$ mm^3 and polished with 0.25 μm diamond paste. Prior to electroless plating, the Cu plates were immersed in hydrochloric acid for 30 s to remove the oxides. The electroless Ni(P) layers with different thickness (0 μm, 0.1 μm, 0.5 μm and 1.5 μm) were produced on the prepared Cu plates. The electroless plating temperature was set to be 40 °C, and the composition of electroless Ni(P) plating solution was listed in Table 1. As shown in Fig. 1, the Ni(P) grain had a uniform surface and the average size was eventually kept at ~ 2.5 μm.

Table 1 Composition of the plating bath for Ni(P) electroless plating solution

Components of plating bath	Concentration
$NiSO_4 \cdot 6H_2O$	30 (g/L)
$NaH_2PO_2 \cdot H_2O$	35 (g/L)
$Na_3C_6H_5O_7 \cdot 2H_2O$	30 (g/L)
NH_4Cl	50 (g/L)
$CH_3CH(OH)COOH$	15 (mL/L)

Before soldering, the commercial Sn–58Bi solder was placed on the Cu substrates with Ni(P) plating. The process of reflow soldering was conducted in an infrared-enhanced reflow oven. After reflow soldering at 180 °C for 10 min, four Sn–58Bi/x Ni(P)/Cu ($x = 0$ μm, 0.1 μm, 0.5 μm and 1.5 μm) joint systems were established. Then, all samples for solid aging were isothermally aged at 115 °C for 24, 72, 120 and 240 h. After aging, all samples were cold mounted, ground and polished to expose the cross-sectional microstructure. The microstructure of interfacial IMC was examined by Scanning Electron Microscopy (SEM), and the composition of interfacial IMC was detected by Energy Dispersive Spectroscopy (EDS).

The thickness of IMC layers was measured by using imaging software. And the procedure of analysis was as follows. (a) The widths of SEM image were gauged relative to the scale bar; (b) the total number of image pixels was recorded; (c) the number of pixels in the IMC was counted; (d) the IMC thickness was calculated using the following equation:

$$I = A/B \times C \quad (1)$$

where I denoted the thickness of the IMC, A was the number of pixels in the IMC, B was the number of pixels in the image, and C represented the real height of the image.

3 Results and discussion

Figure 2 showed the microstructure evolution of IMC in the Sn–58Bi/Cu solder joint. It was well known that Bi did not react with Sn and Cu, therefore, Bi atoms segregated at the

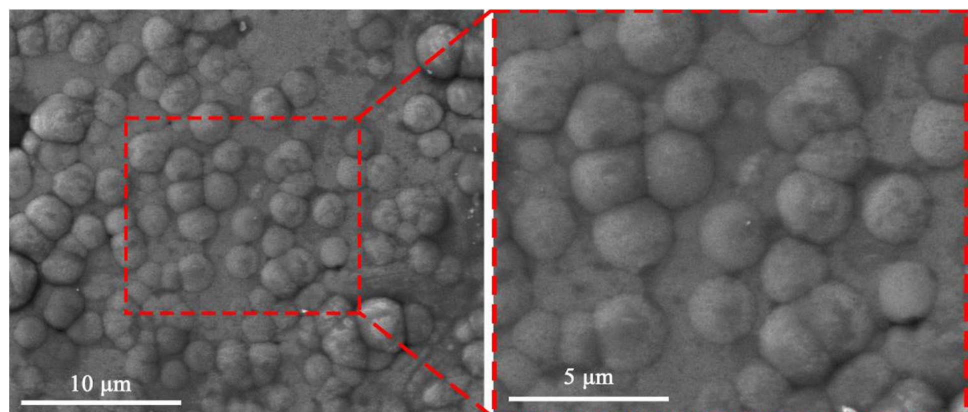

Fig. 1 Microstructure of the Ni(P) grains

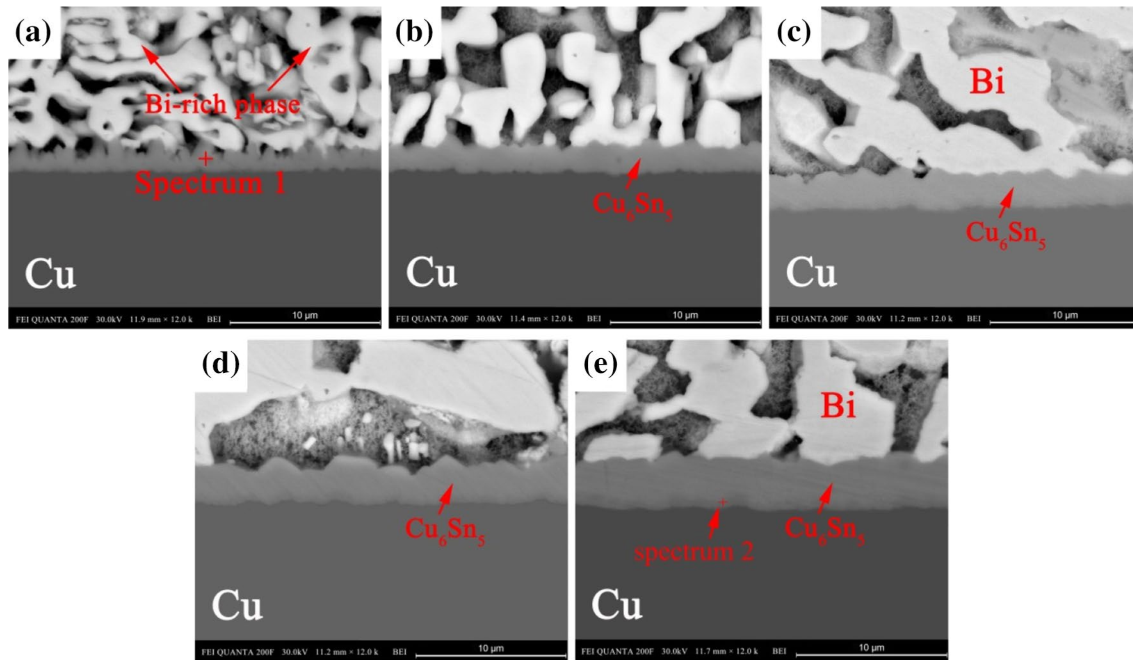

Fig. 2 Microstructure of interfacial IMCs in the Sn–58Bi/Cu solder joint after **a** soldering and solid aging for **b** 24 h, **c** 72 h, **d** 120 h and **e** 240 h

solder matrix to form Bi-rich phase (white phase). The interfacial IMCs marked in Figs. 2a and e were determined by using EDS, and the results were shown in Fig. 3. According to the EDS result, the IMC in Fig. 1a was composed of 53.12 at.% Cu and 46.88 at.% Sn, indicating that the IMC was Cu_6Sn_5. And the IMC in Fig. 2e was composed of 72.77 at.% Cu and 27.23 at.% Sn, indicating that the IMC was Cu_3Sn. It could be found that the Cu_6Sn_5 IMC layer showed the scallop-shape morphology after soldering [22]. Besides, the Cu_6Sn_5 IMC layer in the solder joint would transform from scallop-shape to planar morphology after solid aging for various durations [23–25]. It might be resulted from the low diffusion rate of atoms during aging treatment. After aging for 240 h, the thick Cu_6Sn_5 IMC layer prevented the Sn atom diffusing from solder to substrate. The interfacial reaction transformed from Cu–Sn interaction to Cu–Cu_6Sn_5 interaction, and then a thin Cu_3Sn IMC layer formed between the Cu_6Sn_5 layer and Cu substrate [26].

Figure 4 showed morphologies of interfacial IMCs in the Sn–58Bi/Cu solder joint. It was clear that the Cu_6Sn_5 showed pebble-shape with the smooth surface, and the average dimension of Cu_6Sn_5 grains increased from 0.79 to 2.05 μm. Obvious space could be observed between the Cu_6Sn_5 grains after soldering, as shown in Fig. 4a. However, grains grew by engulfing other grains and the space disappeared after aging for various times. These results were in good agreement with those of previous studies [26–28].

Figure 5 showed the microstructure evolution of interfacial IMC in the Sn–58Bi/0.1 Ni(P)/Cu solder joint. It was clearly found that the 0.1 μm Ni(P) plating was completely consumed after soldering and transformed into Ni_2SnP layer [2, 26]. It has been known that the Ni_2SnP layer was weaker in blocking diffusion than the Ni_3P layer. Thus, it could be found that the IMC layer formed at top and bottom sides of the interface between solder and substrate after soldering. The IMC layers were identified by using EDS, and results showed that the composition of top-side IMC layer was 40.20 at.% Cu, 15.75 at.% Ni and 44.05 at.% Sn, indicating that the IMC was $(Cu,Ni)_6Sn_5$. However, the bottom-side IMC layer was composed of 68.57 at.% Cu, 4.02 at.% Ni and 27.41 at.% Sn, which meant that the bottom-side IMC layer was $(Cu,Ni)_3Sn$. After aging for 24 h, the bottom $(Cu,Ni)_3Sn$ IMC layer reacted with Sn and transformed into $(Cu,Ni)_6Sn_5$ IMC layer. This reaction process could be expressed by the following equation:

$$2Cu_3Sn + 3Sn \rightarrow Cu_6Sn_5 \quad (2)$$

It could be found that the Sn–Cu interaction dominated the reaction profile when the Ni(P) plating thickness was 0.1 μm.

It could be found that the growth rate of $(Cu,Ni)_6Sn_5$ IMC layer on the top side was slower than that on the bottom. It might be the result of different diffusion rates between Sn and Cu [29]. Meanwhile, $(Cu,Ni)_6Sn_5$ IMC layer on the top side showed scalloped-shape even after aging for 240 h. However, it has been reported that the planar-type IMC layer could more effectively prevent subsequent interfacial

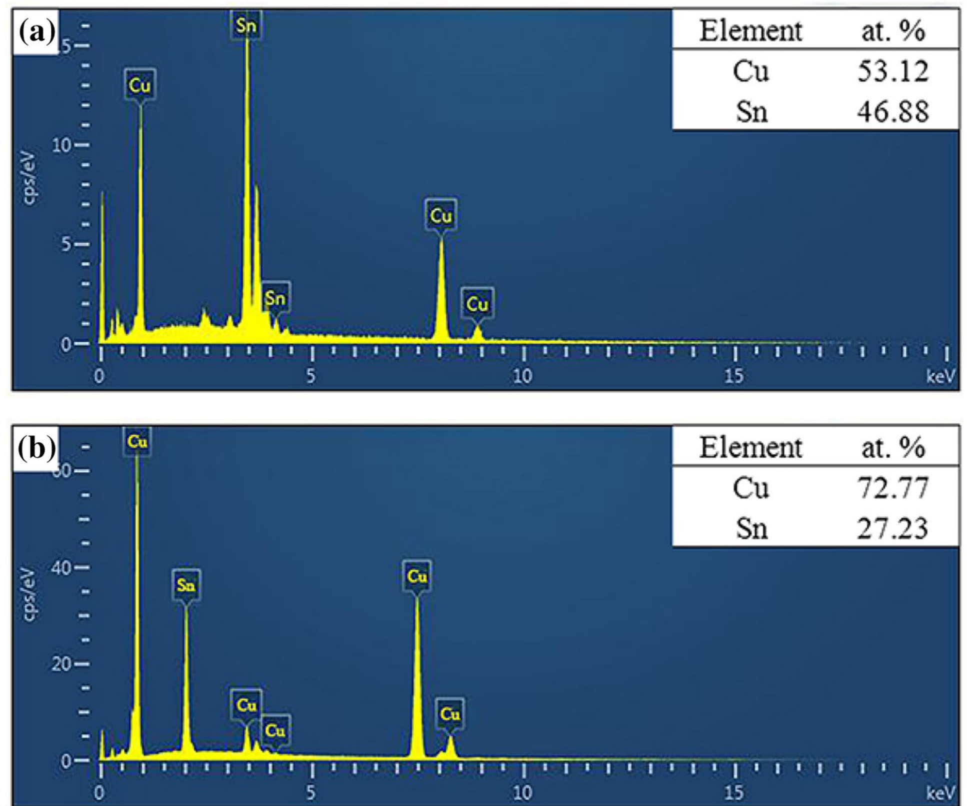

Fig. 3 EDS results of **a** spectrum 1 in Fig. 2a, **b** spectrum 2 in Fig. 2e

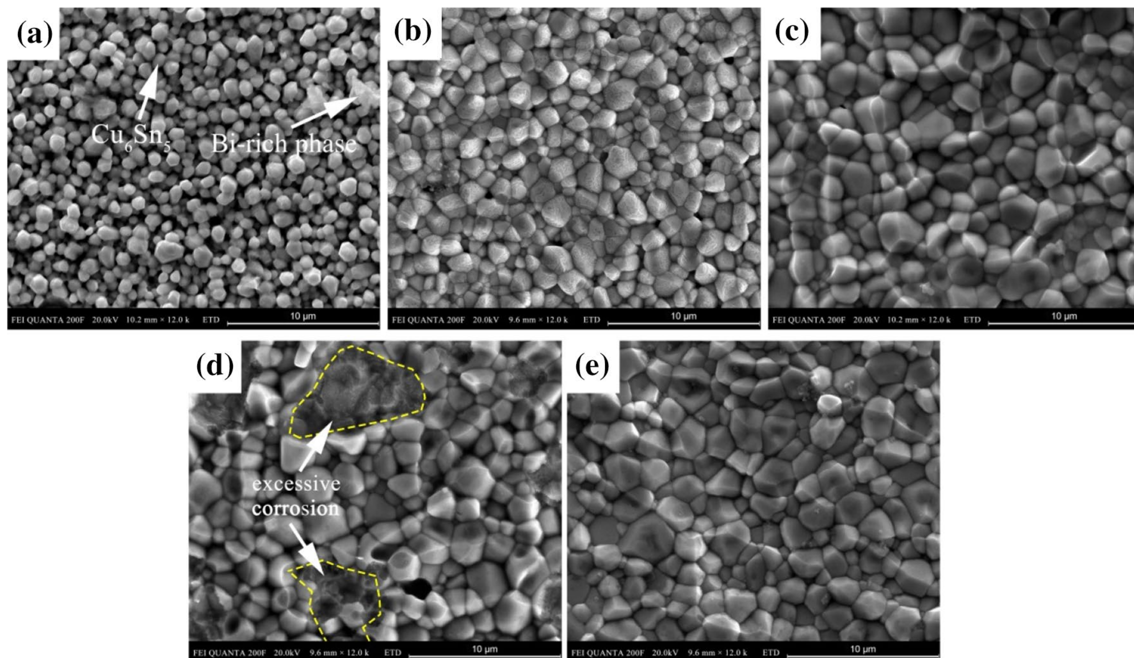

Fig. 4 The top-view SEM images of Sn–58Bi/Cu solder joint after **a** soldering and aging for **b** 24 h, **c** 72 h, **d** 120 h and **e** 240 h

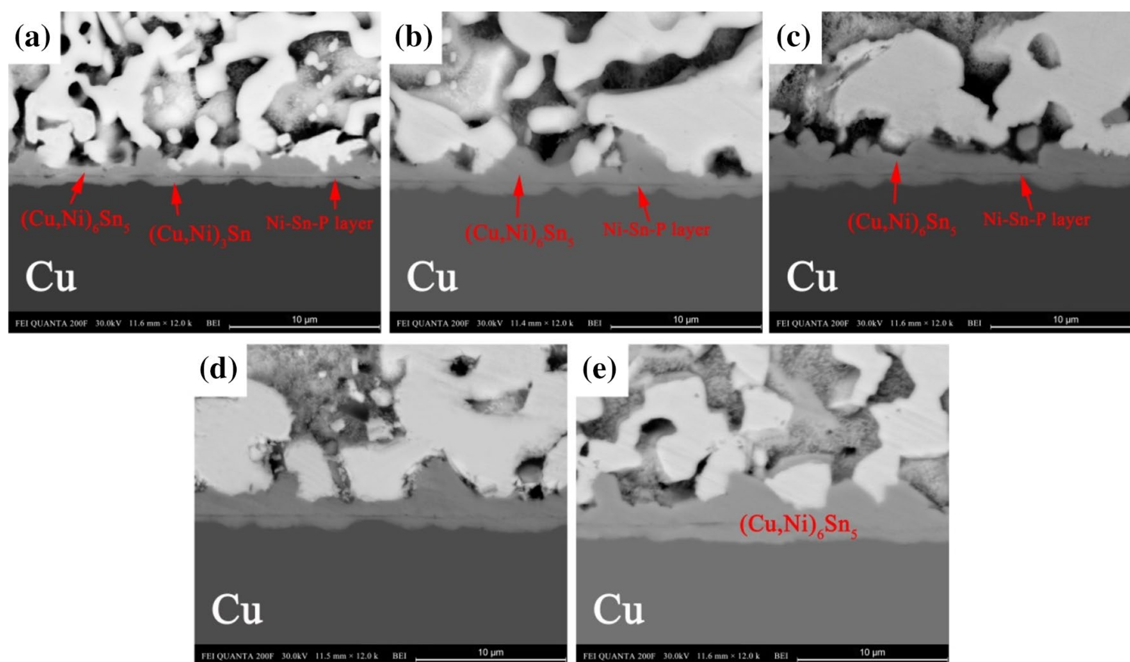

Fig. 5 Microstructure of the interfacial IMC in the Sn–58Bi/0.1 Ni(P)/Cu solder joint after **a** soldering and solid aging for **b** 24 h, **c** 72 h, **d** 120 h and **e** 240 h

reaction between solder and substrate [30]. Besides, the Ni_2SnP layer could significantly decrease the shear strength of the solder joint [31]. However, in Ho's investigation, the structure of Ni–Sn–P IMC layer was confirmed to open up channels for the Sn to diffuse into Cu substrate, thus, indicating that this Ni–Sn–P IMC layer did not function as an efficient diffusion barrier. Thus, it could be concluded that the 0.1 µm Ni(P) plating could not suppress interfacial reactions, and would reduce the mechanical strength of the solder joint.

Figure 6 showed the morphology of interfacial IMC in the Sn–58Bi/0.1 Ni(P)/Cu solder joint. It could be noted that the $(Cu,Ni)_6Sn_5$ showed a needle-type morphology. The difference of morphology was caused by Ni atoms participating into the formation of Cu_6Sn_5 [32–35]. It has been reported that the substitution of Ni for Cu in the interaction process changed the surface energy of $(Cu,Ni)_6Sn_5$ grains [32]. Besides, the needle-type $(Cu,Ni)_6Sn_5$ would transform into chunk-type and hexagonal-type with increase of aging time or Cu content [32, 35]. The large gaps between randomly distributed grains provided fast diffusion channel for atoms between solder and substrate, which also accelerated the formation of IMC layer. This could explain why the $(Cu,Ni)_6Sn_5$ IMC layer on the top side exhibited scallop-type.

Figure 7 showed the microstructure evolution of interfacial IMC in the Sn–58Bi/0.5 Ni(P)/Cu solder joint. It was interesting that the Ni(P) plating remained integrated even after aging for 24 h. It meant that the interfacial reaction was dominated by the Ni–Sn interaction until the solder joint aging for 24 h. Although the Ni(P) plating partly transformed into Ni_2SnP layer after aging for 72 h, only a little solder diffused across the plating and reacted with Cu substrate, as shown in Fig. 7c. And the IMC layer formed at both bottom side and top side at the interface of solder/Ni(P). The composition of top-side IMC was 34.04 at.% Ni, 11.92 at.% Cu and 54.04 at.% Sn, which meant that the IMC layer was $(Ni,Cu)_3Sn_4$. Besides, the bottom-side IMC layer was composed of 69.40 at.% Cu, 3.87 at.% Ni and 26.74 at.% Sn, indicating that the bottom-side IMC layer was $(Cu,Ni)_3Sn$. It meant that the Ni(P) plating acted as an effective diffusion barrier between solder and substrate although it partially transformed into Ni_2SnP layer. Meantime, the top-side IMC layer was consisted of 36.22 at.% Cu, 19.35 at.% Cu and 44.43 at.% Sn, indicating that the IMC layer was $(Cu,Ni)_6Sn_5$.

The Ni atom diffused from the Ni(P) plating and reacted with Sn, and eventually formed a scallop-type IMC layer during soldering, as shown in Fig. 7a. Remarkably, the rate of atomic diffusion was suppressed during aging treatment. The diffusion rate of Ni atoms through the valley was faster than that through the peak, thus the IMC layer showed a planar-type after aging for 24 h. However, the transformation of Ni_2SnP IMC opened the channel of atomic diffusion [15]. Therefore, Sn diffused into the Cu substrate to form a $(Cu,Ni)_3Sn$ layer while Cu diffused to the solder/Ni_3Sn_4 interface to form a $(Ni,Cu)_3Sn_4$ IMC layer. However, the increase of Cu content would be the conversion of IMC from $(Ni,Cu)_3Sn_4$ to $(Cu,Ni)_6Sn_5$ [36].

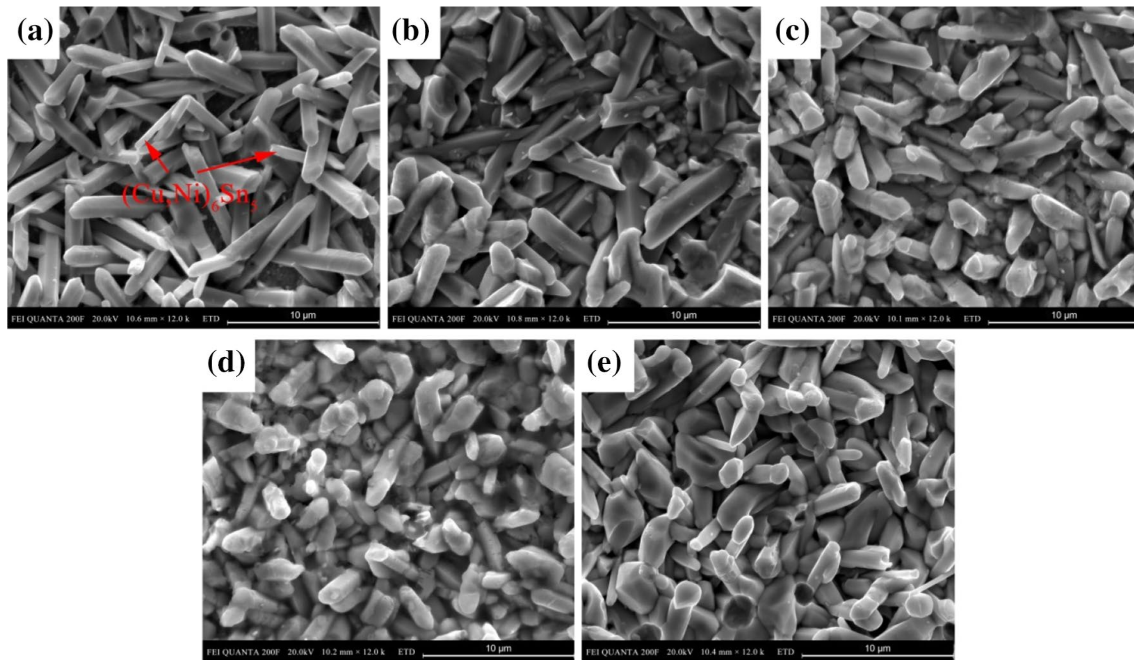

Fig. 6 The top-view SEM images of Sn–58Bi/0.1 Ni(P)/Cu solder joint after **a** soldering and aging for **b** 24 h, **c** 72 h, **d** 120 h and **e** 240 h

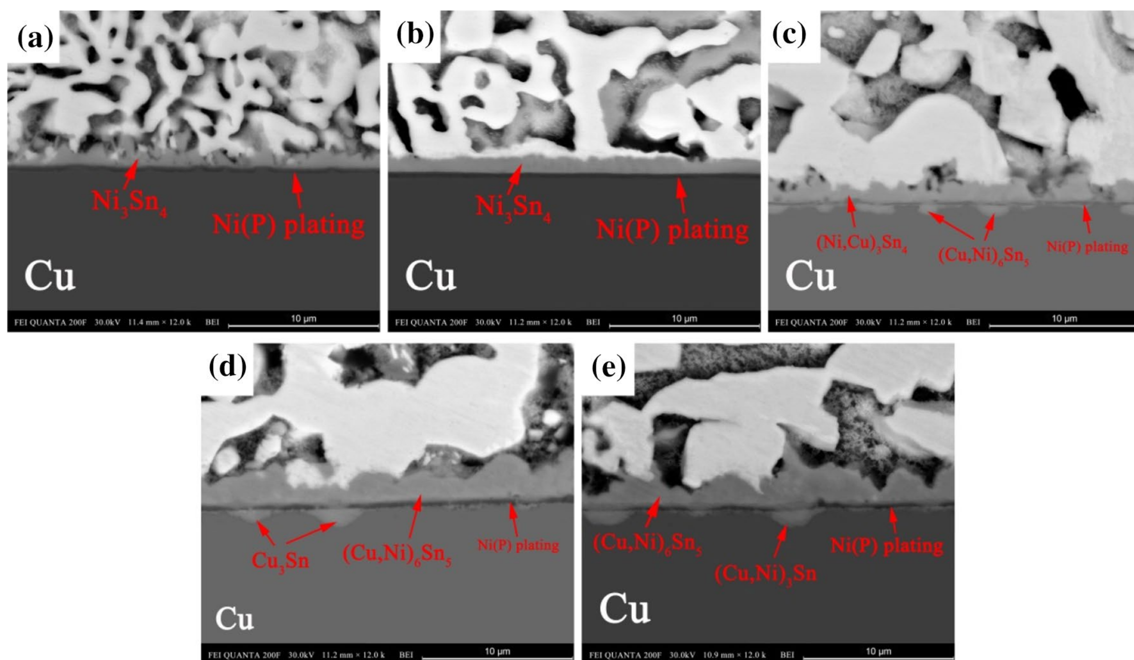

Fig. 7 Microstructure of the interfacial IMC in the Sn–58Bi/0.5 Ni(P)/Cu solder joint after **a** soldering and aging for **b** 24 h, **c** 72 h, **d** 120 h and **e** 240 h

And the conversion process could be express by the following equation:

$$Ni_3Sn_4 + Cu \rightarrow (Cu,Ni)_6Sn_5 \quad (3)$$

Meanwhile, the $(Cu,Ni)_6Sn_5$ IMC layer could act as a diffusion barrier during aging [37]. It was clearly demonstrated that the bottom-side IMC layer hardly grew after the formation of the $(Cu,Ni)_6Sn_5$ IMC layer, as shown in Fig. 7d and e. Thus, it could be concluded that the 0.5 μm Ni(P)

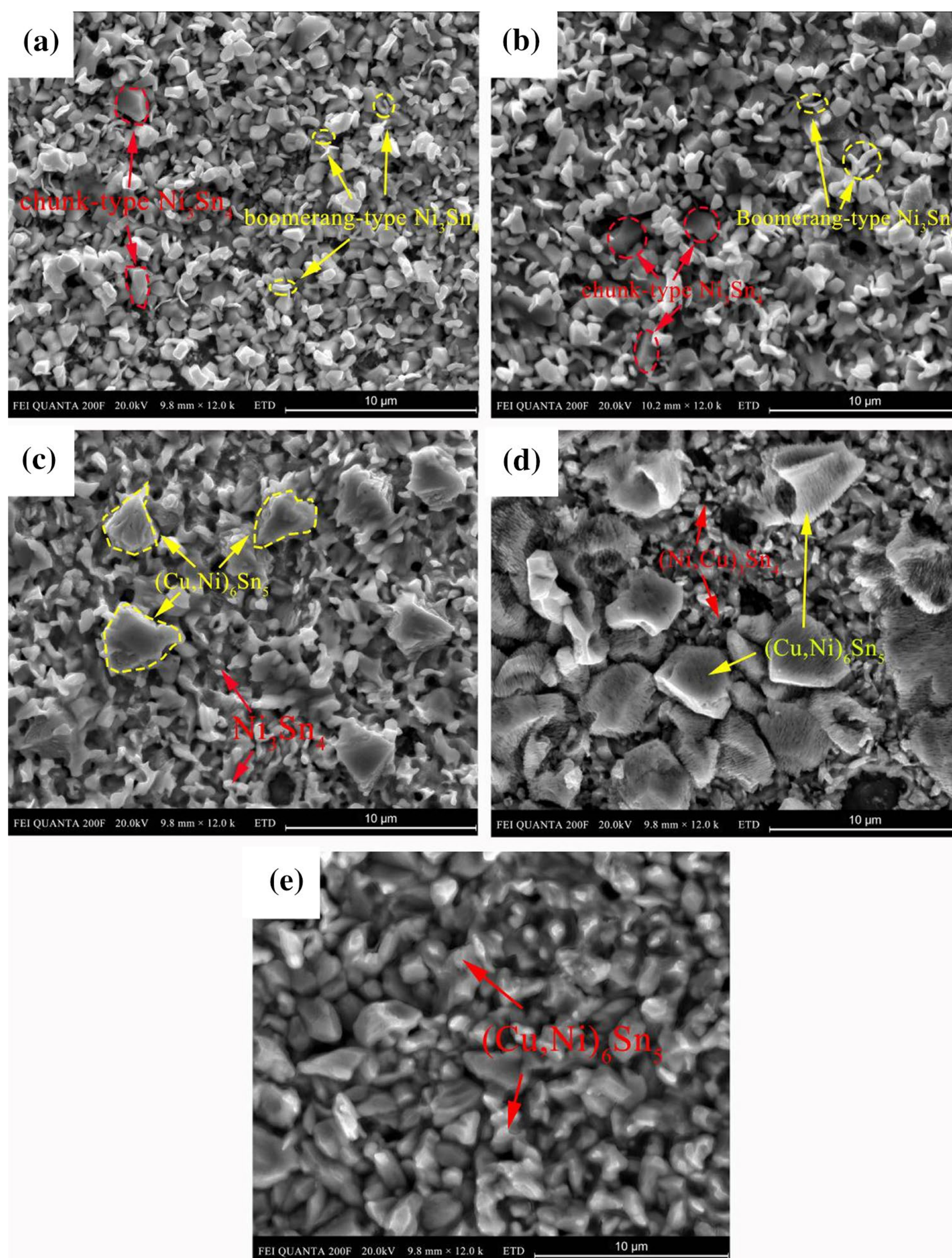

Fig. 8 The top-view SEM images of Sn–58Bi/0.5 Ni(P)/Cu solder joint after **a** soldering and aging for **b** 24 h, **c** 72 h, **d** 120 h and **e** 240 h

plating could work as an effective diffusion barrier between the Sn–58Bi solder and the Cu substrate.

Figure 8 showed the morphology of interfacial IMC in the Sn–58Bi/0.5 Ni(P)/Cu solder joint. It could be found that the Ni_3Sn_4 IMC exhibited two kinds of morphologies: chunk-type and boomerang-type. It had been reported that the boomerang-type Ni_3Sn_4 formed at the short early stage of soldering [38, 39]. Wang and Liu [39] reported that the Ni_3Sn_4 would transform from boomerang-type into chunk-type after soldering for 30 min. However, the boomerang-type Ni_3Sn_4 in this study only increased the grain size but not changed the microstructure. The responsibility for this should be low reaction temperature during the solid aging. However, the boomerang-type Ni_3Sn_4 disappeared after aging for 72 h, which might be the result of growing up [39]. Besides, it could be found that the Ni_3Sn_4 grain transformed into $(Cu,Ni)_6Sn_5$, as marked in Fig. 8c. After the Ni(P) plating partly transformed into Ni_2SnP layer, Cu atoms diffused along the grain boundaries to the Sn/Ni_3Sn_4 interface. The Cu content at the top of the grain gradually increased and eventually caused the transformation of $(Cu,Ni)_6Sn_5$, as described in Eq. 3. The transformation just began after aging for 72 h, which was the reason why the IMC layer was identified as $(Ni,Cu)_3Sn_4$ in Fig. 7c. After that, the Cu-Sn interaction dominated the interfacial reaction. And the $(Cu,Ni)_6Sn_5$ IMC layer formed at the interface

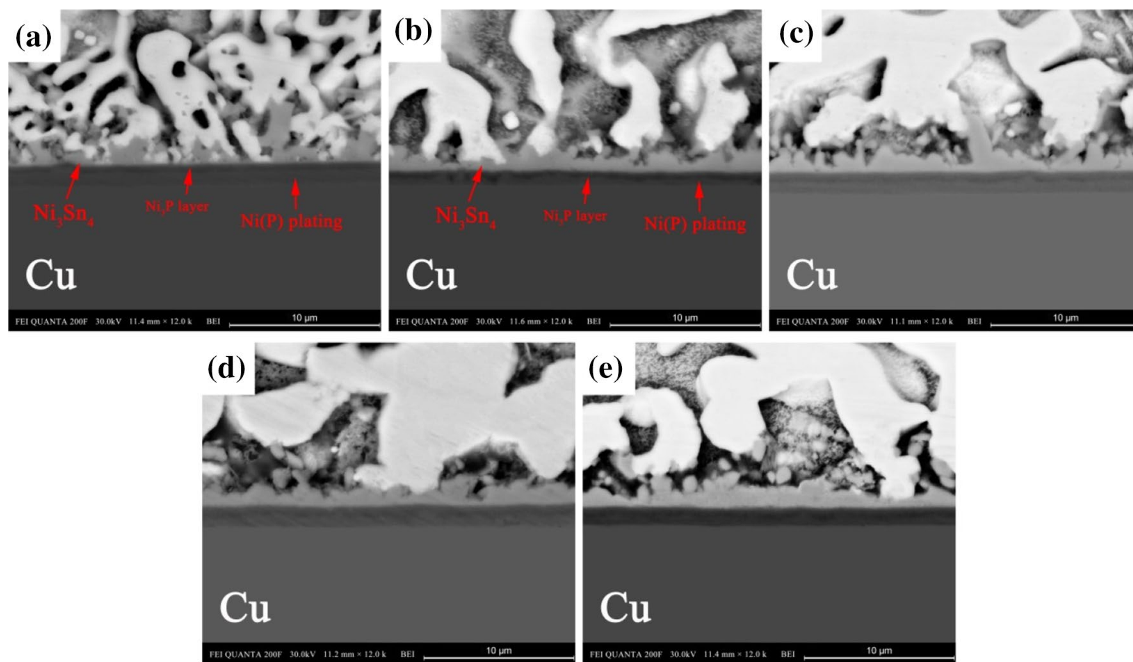

Fig. 9 Microstructure of the interfacial IMC in the Sn–58Bi/1.5 Ni(P)/Cu solder joint after **a** soldering and aging for **b** 24 h, **c** 72 h, **d** 120 h and **e** 240 h

was replaced with $(Ni,Cu)_3Sn_4$ with increase of aging time, as shown in Fig. 8c–e.

Figure 9 showed the microstructure evolution of interfacial IMC in the Sn–58Bi/1.5 Ni(P)/Cu solder joint. It could be clearly found the Ni(P) plating with sufficient thickness even after aging for 240 h. Naturally, the interfacial reaction in solder joint was the Ni–Sn interaction throughout aging process. Ni atom diffused from the Ni(P) plating and reacted with Sn. And the Ni_3Sn_4 IMC layer transformed from scallop-type into planar-type as aging time increased, as shown in Fig. 9a–e. Besides, the P atom in Ni(P) plating was accumulated at the interface of Ni_3Sn_4/Ni(P) plating and reacted with Ni to form a Ni_3P layer [12, 40, 41]. It could be noted that the Ni(P) plating hardly consumed during the solid aging. Indeed, a thick Ni(P) plating could effectively inhibit atom diffusion between the solder and substrate. However, excessive thick Ni(P) plating not only hindered the fine-pitch packaging application, but also reduced reliability of electrical signals [15–17]. Besides, the excessive thickness also increased the cost and created unnecessary waste. Thus it was suggested that the 1.5 μm Ni(P) plating was over-thick in this study.

Figure 10 showed morphologies of interfacial IMCs in the Sn–58Bi/1.5 Ni(P)/Cu solder joint. It could be found that the Ni_3Sn_4 IMCs also showed chunk-type and boomerang-type, which was similar to those in Fig. 8a. However, the boomerang-type Ni_3Sn_4 grains grew and transformed into chunk-type with increase of aging time, as shown in Fig. 10b and c [39]. Meanwhile, the chunk-type grains hardly grew during aging. It might be the result of thick Ni(P) plating acting as an effective diffusion barrier between the solder and substrate. The transformation of $(Cu,Ni)_6Sn_5$ could not be found in the Sn–58Bi/1.5 Ni(P)/Cu solder joint, which meant that the transformation in the Sn–58Bi/1.5 Ni(P)/Cu solder joint was driven by the Cu diffusing through the Ni_2SnP layer.

Figure 11 showed the schematic of interfacial IMC evolution in soldering systems. Pebble-type Cu_6Sn_5 grains initially formed at the interface of Sn–58Bi/Cu solder joint, as represented in region I. And with increase of aging time, the pebble-type Cu_6Sn_5 grains gradually grew and their morphologies would not change. However, as the thickness of Ni(P) plating increased, Ni atoms participated in the IMC formation and changed the morphology of IMC grains. Needle-type $(Cu,Ni)_6Sn_5$ grains formed at the interface of Sn–58Bi/0.1 Ni(P)/Cu solder joint, as revealed in region II [32, 42]. Although it had been reported that the needle-type $(Cu,Ni)_6Sn_5$ grains would transformed into hexagonal-type [32, 34, 43], the morphology of needle-type $(Cu,Ni)_6Sn_5$ grains did not change in this study, which was caused by the low aging temperature and low Ni concentration. When the thickness of Ni(P) plating increased to more than 0.5 μm, the Ni–Sn interaction dominated the interfacial reaction. It could be found that chunk-type Ni_3Sn_4 and boomerang-type Ni_3Sn_4 were formed at the interface between solder and Ni(P) plating, as described in region V. However, the boomerang-type Ni_3Sn_4 grains grew and transformed into chunk-type with increase of aging time [39], as shown in Fig. 10a–c. And this

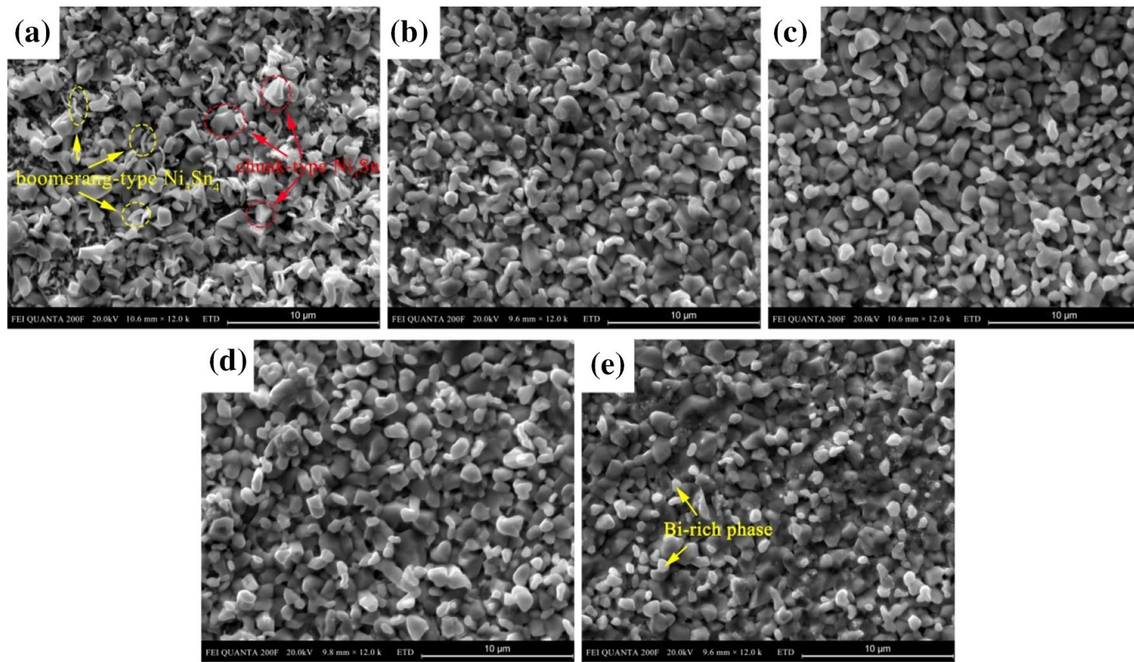

Fig. 10 The top-view SEM images of Sn–58Bi/1.5 Ni(P)/Cu solder joint after **a** soldering and aging for **b** 24 h, **c** 72 h, **d** 120 h and **e** 240 h

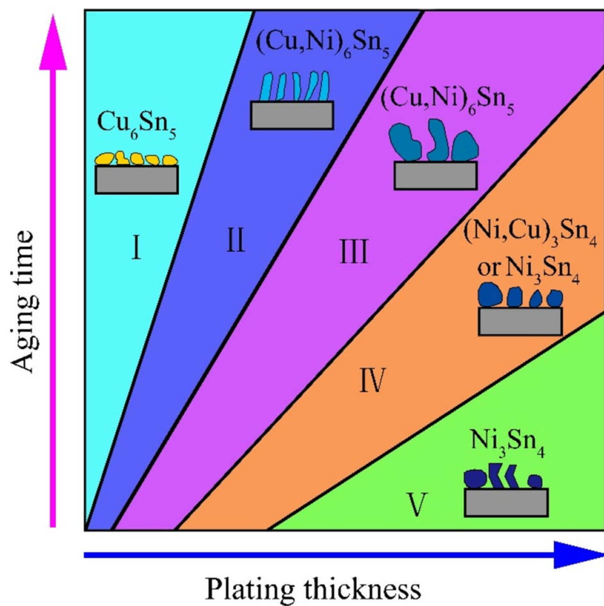

Fig. 11 Schematic of interfacial IMC evolution in solder joints

process was illustrated in region IV. It could be concluded from Fig. 8c that $(Ni,Cu)_3Sn_4$ grains remained chunk-type even though some Ni atom was substituted by Cu atoms. However, more Cu atoms diffused from the substrate and changed the ratio of Cu and Ni at the interface when channels appeared in the Ni_2SnP layer, which caused the transformation of $(Cu,Ni)_6Sn_5$. This transition process could be presented by region III and region IV in Fig. 11.

In order to investigate kinetics of IMC growth, thicknesses of IMC layers in this study were measured using Eq. 1, as demonstrated in Table. 2. According to Kim et al. [44], the growth behavior of IMCs generally followed the line or parabola type during the solid-state aging. The growth rate was controlled by reaction rate when the IMC growth follows the linear kinetics, whereas parabolic growth kinetics implies that the IMC growth was controlled by volume diffusion. It could be found that the growth behavior of IMC in this study followed a parabolic type. In other words, all IMCs growths were controlled by volume diffusion during solid-state aging in this study.

Table 2 Results of the mean IMC thickness of solder systems in this study during aging

Aging time (h)		0	24	72	120	240
Total IMC thickness in different solder joint (μm)	Sn–58Bi/Cu	1.57	1.96	2.40	2.80	3.43
	Sn–58Bi/0.1 Ni(P)/Cu	1.49	1.74	3.34	2.42	3.06
	Sn–58Bi/0.5 Ni(P)/Cu	1.03	1.09	1.53	1.87	2.12
	Sn–58Bi/1.5 Ni(P)/Cu	0.94	1.07	1.27	1.28	1.30

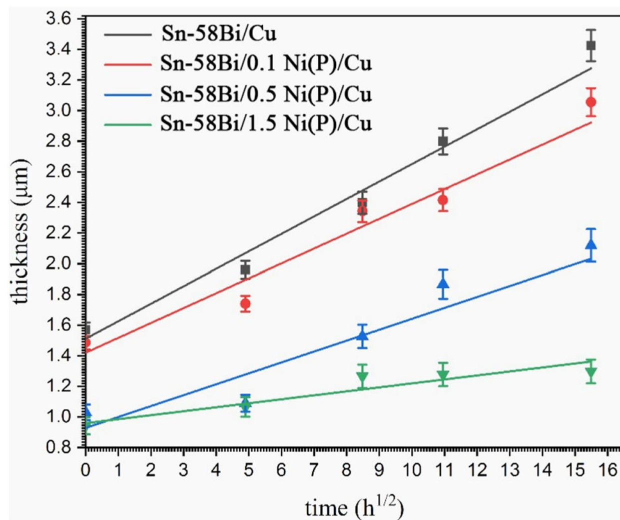

Fig. 12 The relationship between the IMC thickness growth and square root of the solid aging time

The thickness of the IMC layer growth during solid aging condition could be expressed by the following equation [45]:

$$Y = At^n + B \quad (4)$$

where Y was the thickness of IMC layer at time t, B was the initial thickness of the IMC layer after reflow soldering, A was the IMC growth rate constant and n denoted the time exponent. It has been reported that the time exponent n varied from 0.3 [46, 47] to 0.5 [48–50], and even to 0.6 [50]. The IMC growth in this study occurred at solid aging stage, which suggested that the IMC growth was controlled by volume diffusion. Thus, the time exponent n in this study should be equal to 0.5.

Figure 12 showed the relationship between the IMC thickness growth and the square root of solid aging time. It was shown that the IMC growth kinetics of Sn–58Bi/Cu solder joint, Sn–58Bi/0.1 Ni(P)/Cu solder joint, Sn–58Bi/0.5 Ni(P)/Cu solder joint and Sn–58Bi/1.5 Ni(P)/Cu solder joint were 0.114 μm/h$^{1/2}$, 0.097 μm/h$^{1/2}$, 0.071 μm/h$^{1/2}$, and 0.026 μm/h$^{1/2}$, respectively. Both the thickness and growth kinetic of the IMC layer in the Sn–58Bi/Cu solder joint were much larger than those in Sn–58Bi/Ni(P)/Cu solder systems, regardless of the Ni(P) plating thickness, so it could be attributed to the diffusion barrier of Ni(P) plating. Nevertheless, although the growth rate of IMC layer in Sn–58Bi/1.5 Ni(P)/Cu solder joint was the lowest, excessive Ni(P) layer was observed after aging treatment, which suggested that the thickness of this diffusion barrier could be decreased properly. On the other hand, the Ni(P) barrier would be almost consumed after aging for 72 h, thus it could be concluded that the appropriate thickness of Ni(P) plating should be controlled at 0.5–1.5 μm.

4 Conclusion

In this study, the microstructure evolution of interfacial IMCs in Sn–58Bi/x Ni(P)/Cu solder joints (x = 0 μm, 0.1 μm, 0.5 μm and 1.5 μm) were investigated after soldering and solid-state aging for various duration. It was found that the 0.1 μm Ni(P) plating was rapidly consumed after soldering and completely transformed into Ni_2SnP layer. This Ni_2SnP layer could not be efficient in inhibiting the atomic diffusion, and would degrade the reliability. Besides, the grain formed at the interface was needle-type $(Cu,Ni)_6Sn_5$. The Ni–Sn interaction dominated the interfacial reaction when the thickness of Ni(P) plating increased to 0.5 μm. However, the Ni(P) plating partly transformed into Ni_2SnP after aging for 72 h. After that, Cu atoms diffused through the plating and participated into the interaction. The chunk-type Ni_3Sn_4 and boomerang-type Ni_3Sn_4 transformed into chunk-type $(Cu,Ni)_6Sn_5$ in Sn–58Bi/0.5 Ni(P)/Cu solder joint, while the IMC layer forming in the Sn–58Bi/1.5 Ni(P)/Cu solder joint was always Ni_3Sn_4 during the aging process. Although the growth rate of IMC layer in Sn–58Bi/1.5 Ni(P)/Cu solder joint was the lowest, excessive Ni(P) layer was observed after aging treatment, which suggested that the thickness of this diffusion barrier could be decreased properly, and it concluded that the appropriate thickness of Ni(P) plating should be controlled at 0.5–1.5 μm.

Acknowledgements This work was supported by the National Natural Science Foundation of China (No. 51765040), Natural Science Foundation of Jiangxi Province (20192ACB21021), Outstanding Young talents funding of Jiangxi Province (20192BCB23002), the Innovative Funding for Graduate Students in Nanchang University (No. CX2019065) and the State Key Laboratory of Advanced Technologyies for Comprehensive Utilization of Platinum Metals (No. SKL-SPM-202022).

Compliance with ethical standards

Conflict of interest The authors declare that they have no known competing financial interests or personal relationships that could have appeared to influence the work reported in this paper.

References

1. X.Y. Bi, X.W. Hu, X.X. Jiang, Q.L. Li, Effect of Cu additions on mechanical properties of Ni_3Sn_4-based intermetallic compounds: first-principles calculations and nano-indentation measurements. Vacuum **164**, 7–14 (2019)
2. C.-Y. Ho, J.-G. Duh, Quantifying the dependence of Ni(P) thickness in ultrathin-ENEPIG metallization on the growth of CueSn intermetallic compounds in soldering reaction. Mater. Chem. Phys. **148**, 21–27 (2014)
3. X.Y. Bi, X.W. Hu, Q.L. Li, Investigations on elastic properties and electronic structures of α-$CoSn_3$ doped with Ni via first-principles calculations and nano-indentation measurements. Results Phys. **15**, 102607 (2019)

4. X.W. Hu, H. Qiu, X.X. Jiang, Effect of Ni addition into the Cu substrate on the interfacial IMC growth during the liquid-state reaction with Sn–58Bi solder. J. Mater. Sci.: Mater Electron. **30**, 1907–1918 (2019)
5. K. Chung, Y.J. Chen, C.C. Li, C.R. Kao, The critical oxide thickness for Pb-free reflow soldering on Cu substrate. Thin Solid Films **20**, 5346–5352 (2012)
6. W. Yang, J.Y. Wu, Z.X. Zhu, C.R. Kao, Effects of surface diffusion and reaction-induced volume shrinkage on morphological evolutions of micro joints. Mater. Chem. Phys. **191**, 13–19 (2017)
7. J. Wang, S. Xue, P. Zhang, P. Zhai, Y. Tao, The reliability of lead-free solder joint subjected to special environment: a review. J. Mater. Sci.: Mater. Electron. **30**, 9065–9086 (2019)
8. W. Seo, Y.-H. Ko, Y.-H. Kim, S. Yoo, Void fraction of a Sn-Ag-Cu solder joint underneath a chip resistor and its effect on joint strength and thermomechanical reliability. J. Mater. Sci.: Mater. Electron. **30**, 15889–15896 (2019)
9. X. Hu, X. Yu, Y. Li, Q. Huang, Y. Liu, Z. Min, Effect of strain rate on interfacial fracture behaviors of Sn-58Bi/Cu solder joints. J. Mater. Sci. Mater. Electron. **25**, 57–64 (2014)
10. H.Y. Qiu, X.W. Hu, X.X. Jiang, Q.L. Li, The effects of Ni addition on microstructure evolution and mechanical properties of solder joints undergoing solid-liquid electromigration. Mater. Lett. **256**, 126609 (2019)
11. X. Deng, G. Piotrowski, J.J. Williams, N. Chawla, Influence of initial morphology and thickness of Cu_6Sn_5 and Cu_3Sn intermetallics on growth and evolution during thermal aging of Sn-Ag solder/Cu joints. J. Electron. Mater. **32**, 1403–1413 (2003)
12. P. Liu, P. Yao, J. Liu, Effects of multiple reflows on interfacial reaction and shear strength of SnAgCu and SnPb solder joints with different PCB surface finishes. J. Alloys Compd. **470**, 188–194 (2009)
13. K.N. Tu, K. Zeng, Tin–lead (SnPb) solder reaction in flip chip technology. Mater. Sci. Eng. R.: Rep. **34**, 1–58 (2001)
14. J.-W. Yoon, S.-W. Kim, S.-B. Jung, Effect of reflow time on interfacial reaction and shear strength of Sn-0.7Cu solder/Cu and electroless Ni(P) BGA joints. J. Alloys Compd. **385**, 192–198 (2004)
15. C.E. Ho, C.W. Fan, W.Z. Hsieh, Pronounced effects of Ni(P) thickness on the interfacial reaction and high impact resistance of the solder/Au/Pd(P)/Ni(P)/Cu reactive system. Surf. Coat. Technol. **259**, 244–251 (2014)
16. M. Sano, Y. Tahara, C.-Y. Chen, T.-F. Mark Chang, T. Hashimoto, H. Kurosu, T. Sato, M. Sone, Application of supercritical carbon dioxide in catalyzation and Ni-P electroless plating of nylon 6,6 textile. Surf. Coat. Technol. **302**, 336–343 (2016)
17. C.-Y. Ho, J.-G. Duh, C.-W. Lin, C.-J. Lin, Y.-H. Wu, H.-C. Hong, T.-H. Wang, Microstructural variation and high-speed impact responses of Sn-3.0Ag-0.5Cu/ENEPIG solder joints with ultrathin Ni-P deposit. J. Electron. Mater. **48**, 2724–2732 (2013)
18. Y. Li, Z. Wang, X. Li, X. Hu, M. Lei, Growth behavior of IMCs layer of the Sn–35Bi–1Ag on Cu, Ni–P/Cu and Ni–Co–P/Cu substrates during aging. J. Mater. Sci.: Mater Electron. **30**, 1519–1530 (2019)
19. C.E. Ho, L.H. Hsu, C.H. Yang, T.C. Yeh, P.T. Lee, Effect of Pd(P) thickness on the soldering reaction between Sn–3Ag–0.5Cu alloy and ultrathin-Ni(P)-type Au/Pd(P)/Ni(P)/Cu metallization pad. Thin Solid Films **584**, 257–264 (2015)
20. I.K. Hong, H. Kim, S.B. Lee, Optimization of barrel plating process for electroless Ni–P plating. J. Ind. Eng. Chem. **20**, 3767–3774 (2014)
21. A. Kumar, Z. Chen, S.G. Mhaisalkar, C.C. Wong, P.S. Teo, V. Kripesh, Effect of Ni-P thickness on solid-state interfacial reactions between Sn-3.5Ag solder and electroless Ni-P metallization on Cu substrate. Thin Solid Films **504**, 410–415 (2006)
22. W.-R. Myung, Y. Kim, S.-B. Jung, Mechanical property of the epoxy-contained Sn–58Bi solder with OSP surface finish. J. Alloys Compd. **615**, S411–S417 (2014)
23. M.G. Cho, K.W. Paik, H.M. Lee, S.W. Booh, T.-G. Kim, Interfacial reaction between 42Sn-58Bi solder and electroless Ni-P/immersion Au under bump metallurgy during aging. J. Electron. Mater. **35**, 35–40 (2006)
24. X. Gu, K.C. Yung, Y.C. Chan, Thermomigration and electromigration in Sn-58Bi ball grid array solder joints. J. Mater. Sci.: Mater Electron. **21**, 1090–1098 (2010)
25. T.L. Yang, J.Y. Wu, C.C. Li, S. Yang, C.R. Kao, Low temperature bonding for high temperature applications by using SnBi solders. J. Alloys Compd. **647**, 681–685 (2015)
26. Z. Zhang, X.W. Hu, X.X. Jiang, Y.L. Li, Influences of mono-Ni(P) and dual-Cu/Ni(P) plating on the interfacial microstructure evolution of solder joints. Metall. Mater. Trans. A. **50**, 480–492 (2019)
27. J.X. Cheng, X.W. Hu, X.X. Jiang, Interfacial reaction and IMC growth between Sn-37 Pb and heterogeneous dual-phase substrate. Vacuum **159**, 112–124 (2019)
28. P.T. Vianco, J.A. Rejent, P.F. Hlava, Solid-state intermetallic compound layer growth between copper and 95.5Sn-3.9Ag-0.6Cu solder. J. Electron. Mater. **33**, 991–1004 (2004)
29. M. He, Z. Chen, G. Qi, Solid state interfacial reaction of Sn-37Pb and Sn-3.5Ag solders with Ni-P under bump metallization. Acta Mater. **52**, 2047–2056 (2004)
30. S.-M. Lee, J.-W. Yoon, S.-B. Jung, Interfacial reaction and mechanical properties between low melting temperature Sn-58Bi solder and various surface finishes during reflow reactions. J. Mater. Sci.: Mater. Electron. **26**, 1649–1660 (2015)
31. C.E. Ho, T.T. Kuo, W. Gierlotka, F.M. Ma, Development and evaluation of direct deposition of Au/Pd(P) bilayers over Cu pads in soldering applications. J. Mater. Sci. **41**, 3276–3283 (2012)
32. M.L. Huang, F. Yang, Solder size effect on early stage interfacial intermetallic compound evolution in wetting reaction of Sn3.0Ag0.5Cu/ENEPIG joints. J. Mater. Sci. Technol. **31**, 252–256 (2015)
33. C.E. Ho, R.Y. Tsai, Y.L. Lin, C.R. Kao, Effect of Cu concentration on the reactions between Sn-Ag-Cu solders and Ni. J. Mater. Sci. **31**, 584–590 (2002)
34. J.-W. Yoon, S.-W. Kim, S.-B. Jung, Effects of reflow and cooling conditions on interfacial reaction and IMC morphology of Sn–Cu/Ni solder joint. J. Alloys Compd. **415**, 56–61 (2006)
35. M. Huang, F. Yang, N. Zhao, X. Liu, J. Wang, Study on size effect and cross-interaction in Cu/Sn/Ni-P interconnects. Int. Conf. Electron. Packag. Technol. (2014). https://doi.org/10.1109/isaf.2014.6917898
36. J. Li, S.H. Mannan, M.P. Clode, P.P. Conway, Interfacial reaction between molten Sn-Bi based solder and electroless Ni-P coatings for liquid solder interconnects. IEEE Trans. Compon. Packag. Technol. **31**, 574–585 (2008)
37. T. Kadoguchi, N. Take, K. Yamanaka, S. Naga, K. Suganuma, Highly thermostable joint of a Cu/Ni-P plating/Sn-0.7Cu solder added with Cu balls. J. Mater. Sci. **52**, 3244–3254 (2017)
38. M. He, W. HuaLau, G. Qi, Z. Chen, Intermetallic compound formation between Sn-3.5Ag solder and Ni-based metallization during liquid state reaction. Thin Solid Films **462**, 376–383 (2004)
39. C.-H. Wang, J.-L. Liu, Effects of Sn thickness on morphology and evolution of Ni_3Sn_4 grains formed between molten Sn and Ni substrate. Intermetallics **61**, 9–15 (2015)
40. J.W. Jang, D. Frear, D. Frear, T.Y. Lee, K.N. Tu, Morphology of interfacial reaction between lead-free solders and electroless Ni-P under bump metallization. J. Appl. Phys. **88**, 6359–6363 (2000)
41. J.-W. Yoon, S.-W. Kim, S.-B. Jung, IMC morphology, interfacial reaction and joint reliability of Pb-free Sn–Ag–Cu solder on electrolytic Ni BGA substrate. J. Alloys Compd. **392**, 247–252 (2005)

42. J.W. Xian, S.A. Belyakov, T.B. Britton, C.M. Gourlay, Heterogeneous nucleation of Cu6Sn5 in Sn–Cu–Al solders. J. Alloys Compd. **619**, 345–355 (2015)
43. J.-W. Yoon, S.-B. Jung, Interfacial reactions between Sn-0.4Cu solder and Cu substrate with or without ENIG plating layer during reflow reaction. J. Alloys Compd. **396**, 122–127 (2005)
44. D.-G. Kim, S.-B. Jung, Interfacial reactions and growth kinetics for intermetallic compound layer between In-48Sn solder and bare Cu substrate. J. Alloys Compd. **386**, 151–156 (2005)
45. J. Shen, M. Zhao, P. He, Y. Pu, Growth behaviors of intermetallic compounds at Sn-3Ag-0.5Cu/Cu interface during isothermal and non-isothermal aging. J. Alloys Compd. **574**, 451–458 (2013)
46. D. Taneja, M. Volpert, F. Hodaj, Further insight into interfacial interactions in nickel/liquid Sn-Ag solder system at 230–350 °C. J. Mater. Sci. Mater. Electron. **28**, 18366–18378 (2017)
47. J. Shen, Y.C. Chan, S.Y. Liu, Growth mechanism of Ni_3Sn_4 in a Sn/Ni liquid/solid interfacial reaction. Acta Mater. **57**, 5196–5206 (2009)
48. C.-Y. Lin, C.-C. Jao, C. Lee, Y.-W. Yen, The effect of non-reactive alloying elements on the growth kinetics of the intermetallic compound between liquid Sn-based eutectic solders and Ni substrates. J. Alloys Compd. **440**, 333–340 (2007)
49. J. Wang, L.G. Zhang, H.S. Liu, L.B. Liu, Z.P. Jin, Interfacial reaction between Sn-Ag alloys and Ni substrate. J. Alloys Compd. **455**, 159–163 (2008)
50. S.K. Kang, V. Ramachandran, Growth kinetics of intermetallic phases at the liquid Sn and solid Ni interface. Scr. Metall. **14**, 421–424 (1980)

Publisher's Note Springer Nature remains neutral with regard to jurisdictional claims in published maps and institutional affiliations.